Available online at www.sciencedirect.com

SciVerse ScienceDirect

Ceramics International 39 (2013) 6763–6768

CERAMICS INTERNATIONAL

www.elsevier.com/locate/ceramint

Luminescence enhancement of zincblende ZnS:Cl^- nanoparticles synthesized by a low temperature solid state reaction method

Sheng Zhou[a], Yang Li[a], Zhong Chen[a,b], Xiao Xia Li[b], Nan Chen[a], Guoping Du[a,*]

[a]School of Materials Science and Engineering, Nanchang University, Nanchang 330031, China
[b]Institute of Functional Materials, Jiangxi University of Finance & Economics, Nanchang 330013, China

Received 13 January 2013; received in revised form 2 February 2013; accepted 3 February 2013
Available online 11 February 2013

Abstract

Cl^--doped ZnS (ZnS:Cl^-) nanoparticles with strong blue emission were synthesized using a facile low temperature solid state reaction method. X-ray powder diffraction, scanning electron microscopy, UV–vis absorption, and X-ray photoelectron spectroscopy were used to characterize their crystal structures, microstructural characteristics, and chemical compositions, respectively. The ZnS:Cl^- nanoparticles were quasi-spherical in shape and had a cubic zincblende crystal structure. Cl^- doping was found to lead to a reduction in the crystallite size of the ZnS:Cl^- nanoparticles. It showed that Cl^- doping remarkably enhanced the luminescence properties of the ZnS:Cl^- nanoparticles, and an optimal Cl^- doping condition was determined. Post annealing was found to further improve the luminescence properties of the ZnS:Cl^- nanoparticles. The effect of post annealing temperature on the luminescence properties of the ZnS:Cl^- nanoparticles was systematically studied and discussed.

Keywords: ZnS; Nanoparticle; Chlorine doping; Luminescence; Solid state reaction

1. Introduction

In recent years, nanometer-sized materials have become attractive because of their unique characteristics owing to their quantum size confinement and surface effect, which cannot be obtained from bulk materials [1–5]. Among these nanomaterials, II–VI semiconductor materials have received much attention because of their important application prospects in many fields, such as optoelectronics, catalysis and so on.

ZnS, a wide band-gap II–VI semiconductor, has recently attracted a lot of interest due to its promising applications in optoelectronics and catalysis. ZnS has two types of crystal structures, zincblende and wurtzite. The former can be synthesized at relatively low temperature. A lot of work has been done to enhance the optical properties of zincblende ZnS nanomaterials by doping different elements, which are mostly cation ions. Klausch et al. [6] and Kuppayee et al. [7] used a co-precipitation route to synthesize highly luminescent ZnS:Cu nanocrystals, and they found that the emission colors could be adjusted in the range of blue to green by varying the Cu-doping concentration. Yang et al. [8] reported the synthesis of ZnS:M (M = Ag, Cu, Ce and Sn) nanocrystals via microwave irradiation. Hoa et al. [9] employed a hydrothermal method and a chemical solution method, to synthesize Mn-doped ZnS nanoparticles, and they observed enhancement luminescence at room temperature. Prathap et al. [10] studied the Al-doped ZnS films deposited using a chemical precipitation method, and they found that the optical energy band gap decreased slightly with the increase of dopant concentration without significantly affecting the optical transmittance characteristics. Ummartyotin et al. [11] studied the Mn, Cu-doped ZnS powder using a wet chemical synthesis method, and they observed intense tunable emission. Kim et al. [12] reported synthesis of Te-doped ZnS nanowires (NWs) by a thermal chemical vapor deposition method, and they observed blue emission

*Corresponding author. Tel.: +86 791 3969553.
E-mail addresses: guopingdu@ncu.edu.cn, gpdu999@163.com (G. Du).

0272-8842/$ - see front matter © 2013 Elsevier Ltd and Techna Group S.r.l. All rights reserved.
http://dx.doi.org/10.1016/j.ceramint.2013.02.005

with a maximum peak at 440 nm at room temperature. Khani et al. [13] synthesized Fe-doped ZnS quantum dots (QDs) and studied the effect of Fe^{3+} doping concentration on the optical properties of ZnS QDs. Borse et al. [14] used a chemical method to synthesize Pb-doped ZnS nanoparticles and studied the effect of pH value on the photoluminescence (PL) properties of the Pb-doped ZnS nanoparticles. Reddy et al. [15] and Chen et al. [16] used a co-precipitation reaction method to prepare Cr-doped and Mg-doped ZnS nanoparticles, respectively. Pathak et al. [17] synthesized Ba^{2+}-doped ZnS nanoparticles using a precipitation method and they observed an emission redshift from the blue region toward the visible region after Ba^{2+} doping.

Research work has also been devoted to the anion doping for ZnS nanocrystals. Koda and Shionoya [18] and Georgobiani et al. [19] prepared Cl^--doped ZnS single crystals in the 70s and earlier. They found that Cl^- substitutes S^{2-} and acts as an n-type dopant or donor. Akimoto et al. [20] doped O^{2-} into single-crystalline ZnS using the molecular beam epitaxy method, and they found that O^{2-} dopants act as acceptors in ZnS. Manzoor et al. [21] employed a wet-chemical precipitation method to synthesize ZnS nanoparticles codoped with Cu^+ and halogen ions such as F^-, Cl^-, Br^- or I^-, which were supplied by ammonium halogen salts. Shirata et al. [22] synthesized Cl^--doped ZnS phosphors by firing powder mixtures of ZnS with $MgCl_2$ and NaCl at 1100 °C for 3 h.

In this work, instead of using the wet-chemical or the high temperature synthesis methods, we employed a facile low temperature solid state reaction method [23] to synthesize Cl^--doped ZnS (ZnS:Cl^-) nanoparticles, which were found to exhibit a large luminescence enhancement over the undoped ZnS nanoparticles. Recently, O^{2-} and Br^- [24,25] dopants have been found to strongly enhance the luminescence of ZnS nanoparticles synthesized using this method.

2. Experimental

ZnS:Cl^- nanoparticles were prepared by using analytical grade TAA (CH_3CSNH_2), zinc acetate ($C_4H_6O_4Zn \cdot 2H_2O$) and ammonium chloride (NH_4Cl) reagents as the starting materials. TAA, zinc acetate, and NH_4Cl were the source materials for supplying S, Zn, and Cl, respectively, for the ZnS:Cl^- nanoparticles. Firstly, appropriate amounts of the TAA, zinc acetate and NH_4Cl starting materials were weighed. The Cl^- doping concentration x is based on the molecular formula $ZnS_{(1-x)}Cl_x$ [25]. After intimately mixing the starting materials with ethanol, the mixed materials were put in a crucible and kept in an oven at 130 °C for 3 h for the synthesis reaction. It should be noted that the reaction conditions were chosen after a series of optimization for the strongest luminescence of the as-prepared nanoparticles. The product was then dispersed into deionized water, and some precipitates were obtained. The precipitates were retrieved by high-speed centrifugation and washed several times with deionized water and acetone to remove the residues. The washed precipitates were then dried under vacuum at 30 °C for 10 h. Finally, the ZnS:Cl^- nanoparticles were obtained as confirmed by the XRD results in the following section. The Cl^- doping concentration x was chosen as $x=0$, 0.01, 0.02, 0.03, 0.04, 0.05, 0.06, 0.07, and 0.08.

X-ray diffraction (XRD, Bruker D8 Focus) technique was used to study the crystal structures of the ZnS:Cl nanoparticles. The X-ray diffractometer with a graphite monochromatized Cu Kα radiation ($\lambda=0.15406$ nm) was operated at a step of 0.02° in the 2θ from 10° to 80°. Microstructural characteristics were investigated using a field emission scanning electron microscope (FESEM, Hitachi S4800). Photoluminescence spectra were obtained at room temperature using a Hitachi F-4600 fluorescence spectrophotometer with a xenon lamp source.

3. Results and discussion

3.1. Crystal structures and microstructural characteristics

The XRD patterns of the as-synthesized ZnS:Cl^- nanoparticles are shown in Fig. 1a. All the XRD patterns in Fig. 1a can be readily indexed to the cubic zincblende ZnS crystal structure (JCPDS card, no. 77-2100, $a=5.4145$ Å), and no diffraction peaks for any secondary phase were present. It is noted in Fig. 1a that with the increase of Cl^- doping concentration x, the diffraction peaks (111), (220) and (311) consistently shifted to higher angles until $x=0.06$, beyond which no more shift was observed. This implies that there existed a doping limitation for Cl^- ions in ZnS, which is reasonable because Cl^- and S^{2-} ions have different electrical charges and ionic radii. The decrease of lattice constant with x (Fig. 1b) should be a result of Cl^- doping in the ZnS lattice, as Cl^- ion has a smaller radius than S^{2-} ion [26].

It is also noted in Fig. 1b that the crystallinity of the ZnS:Cl^- nanoparticles became poorer with the Cl^- doping concentration x. Two sources of contribution are responsible for this behavior. The first one was originated from the presence of Cl^- dopants, which as impurities in the ZnS lattice can weaken the diffraction peaks of the ZnS:Cl^- nanoparticles. The second one was due to the extra Zn vacancies in the ZnS lattice generated by Cl^- dopants substituting S^{2-} ions [25]. For the requirement of charge neutrality in the ZnS lattice, every two substituting Cl^- ions will create a Zn^{2+} vacancy. This of course will decrease the crystallinity of the ZnS nanocrystals to a certain extent.

The XRD patterns in Fig. 1 can be used to estimate the average crystallite size of the ZnS:Cl^- nanoparticles by using Scherrer's formulae [27],

$$d = 0.89\lambda/\beta\cos\theta \quad (1)$$

where d is the crystallite size, λ is the X-ray wavelength (1.54056 Å), β is the full width at half maximum of the diffraction peak, and θ is the Bragg angle. As shown

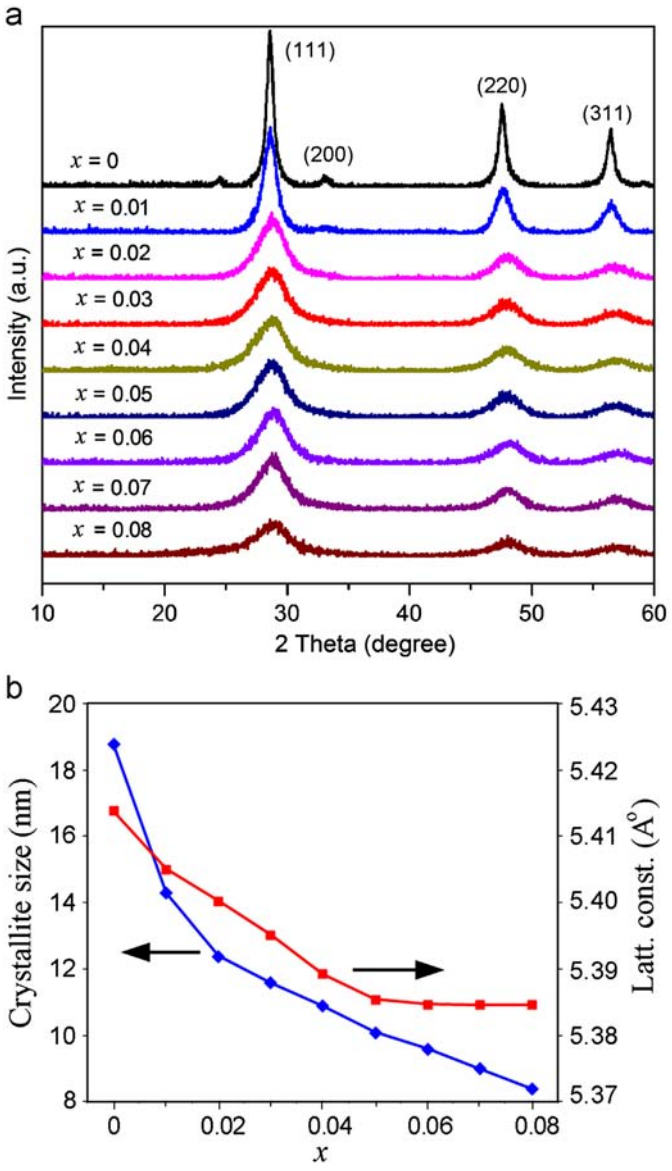

Fig. 1. XRD patterns of the as-synthesized undoped and Cl^--doped ZnS nanoparticles (a), and the dependence of their lattice constant and crystallite size on the Cl^- doping concentration x (b).

in Fig. 1b, with the increasing amount of Cl^- doping, the average crystallite size of the ZnS:Cl^- nanoparticles decreased consistently from 18.8 nm to 8.4 nm. Two possible reasons can explain this behavior. First, the Cl^- dopants can introduce internal strains into the lattice of ZnS:Cl^- nanoparticles, and this will restrict their crystal growth to a certain extent. Secondly, the addition of NH_4Cl in the synthesis reaction might have hindered the diffusion of Zn^{2+} and S^{2-} ions, and therefore restricted the growth of ZnS:Cl^- nuclei, resulting in a smaller crystallite size for the ZnS:Cl^- nanoparticles.

Fig. 2 shows the SEM images of the as-synthesized ZnS and ZnS:Cl^- nanoparticles (x=0.06). The ZnS nanoparticles were well dispersed (Fig. 2a), while the ZnS:Cl^- nanoparticles were agglomerated (Fig. 2b). Both the ZnS and ZnS:Cl^- nanoparticles are roughly spherical in shape.

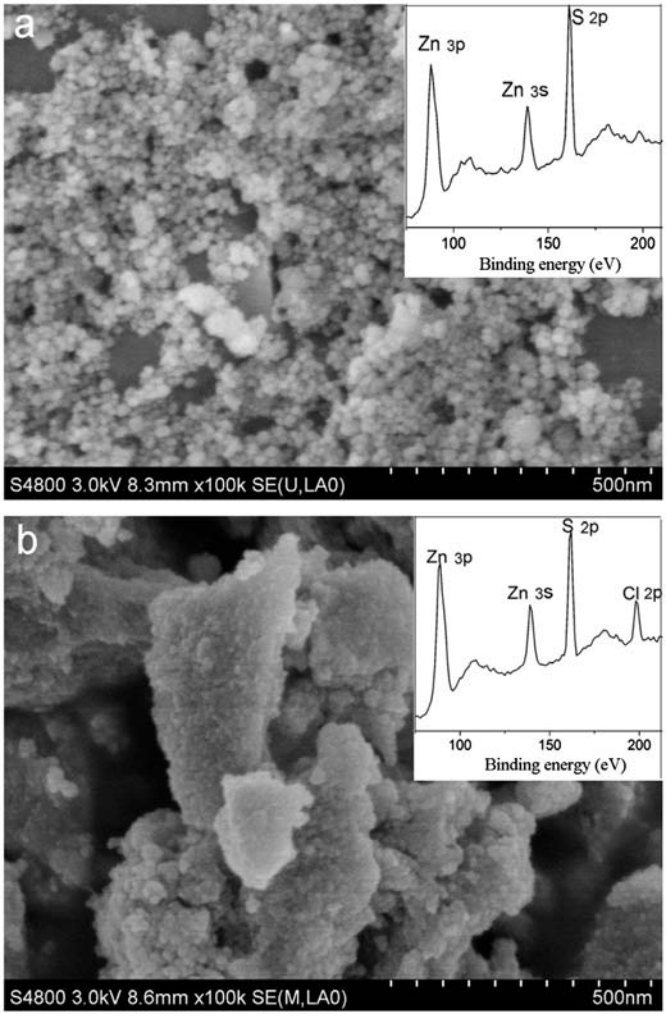

Fig. 2. SEM images of the as-synthesized ZnS (a) and ZnS:Cl^- (x=0.06) (b) nanoparticles. The insets show the XPS spectra.

As shown in Fig. 2a, the particle size of the ZnS nanoparticles was about 20 nm, while the ZnS:Cl^- nanoparticles were about 11 nm in size (Fig. 2b). These measured particle sizes are slightly larger than those estimated from the XRD patterns by using Scherrer's formula (Fig. 1b). This is a result of the presence of crystal defects and internal strains in these nanoparticles, which will slightly broaden XRD peaks [27]. The X-ray photoelectron spectroscopy (XPS) spectra in insets of Fig. 2 confirmed the presence of Cl^- dopants in the ZnS:Cl^- nanoparticles, and the Cl^- doping concentration in the ZnS:Cl^- nanoparticles was estimated to be about 5.6%, which is in good agreement with the intended Cl^- doping concentration x=0.06. Therefore, Cl^- ions were effectively doped into the ZnS nanoparticles.

3.2. Optical properties

Fig. 3 shows the optical absorption spectra of the ZnS nanoparticles and the ZnS:Cl^- nanoparticles with the Cl^- doping concentration at x=0.06. The ZnS nanoparticles showed a strong absorption edge at around 307 nm, and

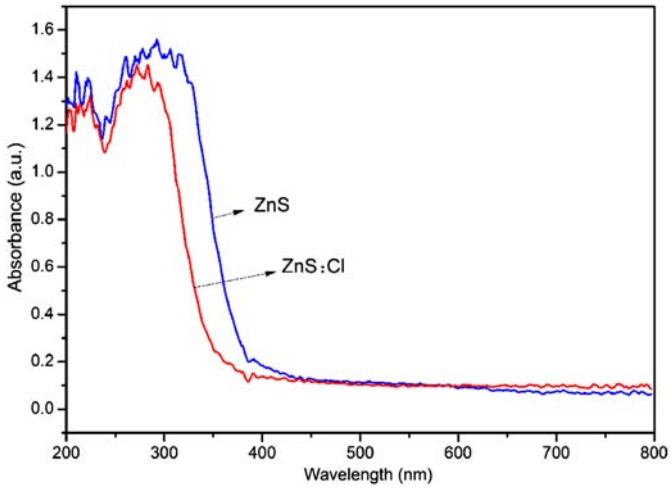

Fig. 3. The UV–vis spectra of the as-synthesized ZnS (a) and ZnS:Cl^- ($x=0.06$) (b) nanoparticles.

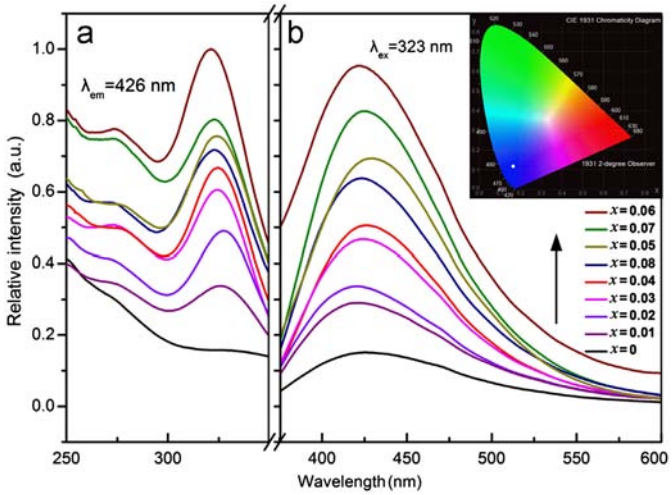

Fig. 4. The excitation (a) and emission (b) spectra of the as-synthesized ZnS and ZnS:Cl^- ($x=0.06$) nanoparticles.

this is shorter than the bulk ZnS materials having an absorption edge at about 338 nm [28]. This blueshift in the absorption edge for the ZnS nanoparticles is a result of the quantum confinement effect [29]. It is also noted in Fig. 3 that the absorption edge of the ZnS:Cl^- nanoparticles was at about 293 nm, indicating a small blueshift from the ZnS nanoparticles (307 nm). This can be explained by the fact that the ZnS:Cl^- nanoparticles had a smaller crystallite size than the ZnS nanoparticles as shown in Fig. 1b and Fig. 2 [30].

The excitation and emission spectra of the as-synthesized ZnS and ZnS:Cl^- nanoparticles are shown in Fig. 4. Two distinct excitation peaks at around 276 nm and 323 nm can be observed from the excitation spectra in Fig. 4a. The intense excitation peak around 276 nm was due to the band to band transition of electrons [31]. The excitation peak at around 323 nm was believed to be originated from the optical absorption by the electrons located at the vacancies V''_{Zn} and the complexes $(V_{Zn}Cl)'$ sites, both of which are acceptor-type defects in the Cl^--doped ZnS [19]. This result is supported by the fact that the intensity of the excitation peak at around 323 nm increased quickly with the Cl^- doping concentration when $x \leq 0.06$ as shown in Fig. 4a. A larger number of Cl^- dopants indicates a higher concentration of Zn vacancies.

It can be seen in Fig. 4b that the intensity of the emission band around 426 nm of the ZnS:Cl^- nanoparticles was significantly increased after doping Cl^- ions, and it is blue emission (see the inset in Fig. 4b). The emission intensity for the ZnS:Cl^- nanoparticles with $x=0.06$ was calculated to be 7 times stronger than the undoped ZnS nanoparticles (Fig. 4b). The emission band around 426 nm was believed to be generated by the defect emission from S^{2-} vacancies [32]. In this process, the photogenerated charge carriers trapped in the shallow traps formed by S^{2-} vacancies emit photons after a radiative recombination with holes in the valence band [33]. The emission enhancement by Cl^- doping in the ZnS nanoparticles can be explained by the fact that Cl^- dopants can create Zn vacancies. As stated in the previous paragraph, these Zn vacancies can improve the excitation intensity (Fig. 4a).

As shown in Fig. 4b, the emission intensity quickly increased with the amount of Cl^- sources in the synthesis reaction until $x=0.06$, and then decreased afterward. It is noted in Fig. 1b that the particle size of the ZnS:Cl^- nanoparticles decreased steadily with the amount of Cl^- sources. For compound semiconductor nanocrystals, it has been known that their luminescence emission intensity strongly depends on their size [34], and it usually increases with the decrease of their particle size [35]. For the ZnS:Cl^- nanoparticles in this work, when the source of Cl^- ions was oversupplied, some of them could form non-radiative recombination centers. This is because, as stated in the previous paragraphs, the doping concentration of Cl^- ions for substituting S^{2-} ions in ZnS nanocrystals is limited. These non-radiative recombination centers will weaken the emission intensity of ZnS:Cl^- nanoparticles for $x > 0.06$ even though their particle sizes were smaller (Fig. 1b).

3.3. Effects of post annealing on the luminescence properties

As stated in Section 3.2, the as-synthesized ZnS:Cl^- nanoparticles with $x=0.06$ exhibited the strongest lunminescence (Fig. 4). Here, we annealed these ZnS:Cl^- nanoparticles in air at different temperatures. Fig. 5 shows the XRD patterns and luminescence spectra of the ZnS:Cl^- nanoparticles annealed for 30 min at different temperatures, 90 °C, 100 °C, 110 °C, 120 °C, and 130 °C. The XRD patterns in Fig. 5a indicate that the annealed ZnS:Cl^- nanoparticles remained to be of cubic zincblende ZnS crystal structure. The crystallinity of the annealed ZnS:Cl^- nanoparticles increased with the annealing temperature. The average particle sizes of the annealed ZnS:Cl^- nanoparticles were calculated by using Scherrer's formulae (Eq. (1)). It is not surprising that their

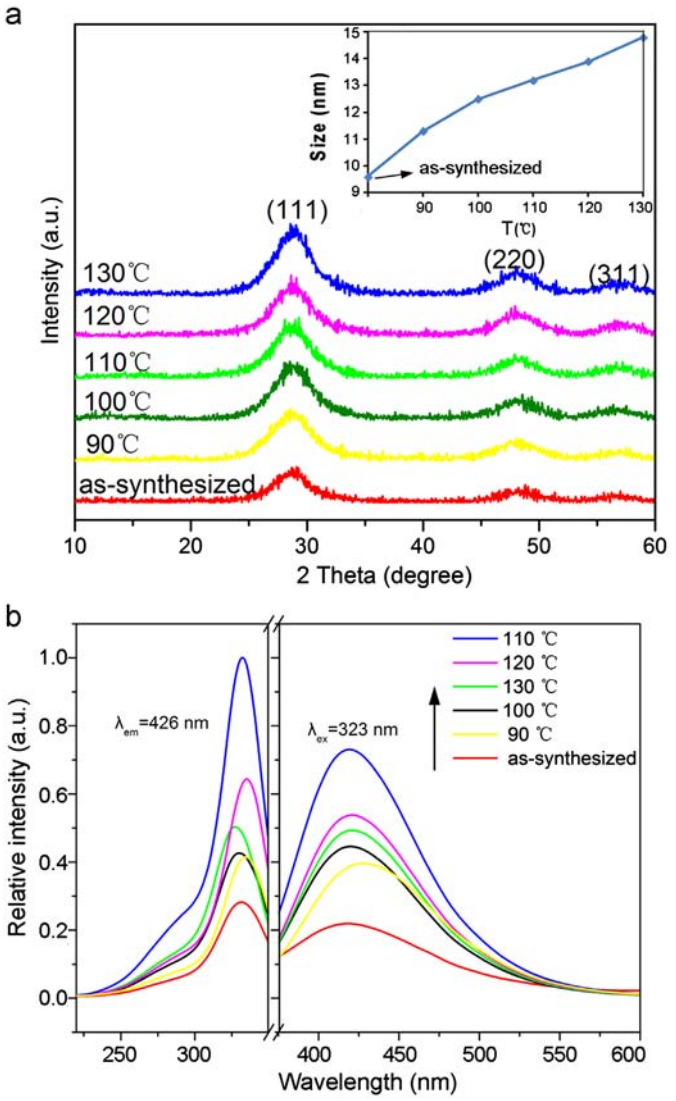

Fig. 5. XRD patterns (a), and excitation (b) and emission (c) spectra of the ZnS:Cl^- ($x=0.06$) nanoparticles annealed for 30 min. The inset shows the dependence of crystallite size on the annealing temperature.

average particle sizes steadily increased after annealing (see the inset of Fig. 5a).

After annealing, the lunminescence intensity of the annealed ZnS:Cl^- nanoparticles was much stronger than the as-synthesized samples (Fig. 5b and c). This suggests that the post annealing has a strong effect in improving the luminescence properties of ZnS:Cl^- nanoparticles. A redshift in the emission spectra caused by the annealing can be clearly observed in Fig. 5c. This is a result of the increased particle size for the annealed ZnS:Cl^- nanoparticles as shown in the inset of Fig. 5a [24,36].

It is also noted in Fig. 5b and c that the lunminescence intensity quickly increased with the annealing temperature until 110 °C, and then decreased afterwards. The ZnS:Cl^- nanoparticles annealed at 110 °C had an emission intensity about 3 times higher than the as-synthesized ZnS:Cl^- nanoparticles. During annealing, 2 factors are believed to influence the luminescence of ZnS:Cl^- nanoparticles. One is the defect structures which will be changed during the annealing process. Defects in ZnS nanoparticles play a key role in their luminescence properties [37]. The other factor is the particle size of the ZnS:Cl^- nanoparticles, where the quantum confinement effect and surface effect can largely intensify their luminescence emission [31]. These two factors compete with each other for the annealed ZnS:Cl^- nanoparticles. On one hand, some of the defects which act as non-radiative recombination centers in the ZnS:Cl^- nanoparticles were eliminated by annealing, and this will improve the emission intensity. One the other hand, the particle size of the ZnS:Cl^- nanoparticles will increase after annealing, and the emission intensity will become lower due to the larger particle size [37]. Because of these two competing factors, an optimal annealing condition for the strongest luminescence emission should therefore be expected. This explains the dependence of the luminescence properties of the ZnS:Cl^- nanoparticles on the annealing temperature as shown in Fig. 5b and c.

4. Conclusions

In summary, we successfully synthesized ZnS:Cl^- nanoparticles with strong blue emission using the low temperature solid state reaction method. The ZnS:Cl^- nanoparticles were quasi-spherical in shape and had a cubic zincblende crystal structure. The crystallite size of the ZnS:Cl^- nanoparticles decreased with the Cl^- doping concentration. It was shown that Cl^- doping remarkably enhanced the luminescence properties of the ZnS:Cl^{--} nanoparticles. An optimal Cl^- doping condition was determined, and the emission intensity of the ZnS:Cl^- nanoparticles was enhanced by as much as 7 times. Post annealing was found to further improve the luminescence properties of the ZnS:Cl nanoparticles. The optimal annealing temperature was about 110 °C, and the emission intensity was increased by 3 times after such annealing. This work indicates that Cl^--doped ZnS nanoparticles with strong blue emission can be readily synthesized using the low temperature solid state reaction method.

Acknowledgments

This work was supported by the Natural Science Foundation of China (61204003), the Natural Science Foundation of Jiangxi Province (2010GQS0064), and the Program for Innovative Research Team of Nanchang University.

References

[1] Y.L. Soo, Z.H. Ming, S.W. Huang, Y.H. Kao, Local structures around Mn luminescent centers in Mn-doped nanocrystals of ZnS, Physical Review B 50 (1994) 7602–7607.

[2] P. Yang, M. Lü, D. Xü, D. Yuan, G. Zhou, Photoluminescence properties of ZnS nanoparticles co-doped with Pb^{2+} and Cu^{2+}, Physics Letters 336 (2001) 76–80.

[3] S. Lu, B. Lee, Z. Wang, W. Tong, B. Wanger, W. Park, C. Summers, Synthesis and photoluminescence enhancement of Mn^{2+}-doped ZnS nanocrystals, Journal of Luminescence 92 (2000) 73–78.
[4] H. Kachkachi, A. Ezzir, M. Nogues, E. Tronc, Surface effects in nanoparticles: application to maghemite γ-Fe_2O_3, European Physical Journal B 14 (2000) 681–689.
[5] A. Becheri, M. Dürr, P. Nostro, P. Baglioni, Synthesis and characterization of zinc oxide nanoparticles: application to textiles as UV-absorbers, Journal of Nanoparticle Research 10 (2008) 679–689.
[6] A. Klausch, H. Althues, C. Schrage, P. Simon, A. Szatkowski, M. Bredol, D. Adam, S. Kaskel, Preparation of luminescent ZnS:Cu nanoparticles for the functionalization of transparent acrylate polymers, Journal of Luminescence 130 (2010) 692–697.
[7] M. Kuppayee, G.K. Vanathi, V. Ramasamy, Enhanced photoluminescence properties of ZnS:Cu^{2+} nanoparticles using PMMA and CTAB surfactants, Materials Science in Semiconductor Processing 15 (2012) 136–144.
[8] H. Yang, C. Huang, X. Su, A. Tang, Microwave-assisted synthesis and luminescent properties of pure and doped ZnS nanoparticles, Journal of Alloys and Compounds 402 (2005) 274–277.
[9] T. Hoa, N. The, S. Mcvittie, N. Nam, L. Vu, T. Canh, N. Long, Optical properties of Mn-doped ZnS semiconductor nanoclusters synthesized by a hydrothermal process, Optical Materials 33 (2011) 308–314.
[10] P. Prathap, N. Revathi, Y.P.V. Subbaiah, K.T. Ramakrishna Reddy, R.W. Miles, Preparation and characterization of transparent conducting ZnS:Al films, Solid State Sciences 11 (2009) 224–232.
[11] S. Ummartyotin, N. Bunnak, J. Juntaro, M. Sain, H. Manuspiya, Synthesis and luminescence properties of ZnS and metal (Mn, Cu)-doped-ZnS ceramic powder, Solid State Sciences 14 (2012) 299–304.
[12] S. Kim, T. Lim, M. Jung, Ki-Jeong. Kong, S. Ju, Bright blue emission from Te-doped ZnS nanowires, Journal of Luminescence 130 (2010) 2153–2156.
[13] O. Khani, H.R. Rajabi, M.H. Yousefi, A.A. Khosravi, M. Jannesari, M. Shamsipur, Synthesis and characterizations of ultra-small ZnS and $Zn_{(1-x)}Fe_xS$ quantum dots in aqueous media and spectroscopic study of their interactions with bovine serum albumin, Spectrochimica Acta A: Molecular and Biomolecular Spectroscopy 79 (2011) 361–369.
[14] P. Borse, W. Vogel, S.K. Kulkarni, Effect of pH on photoluminescence enhancement in Pb-doped ZnS nanoparticles, Journal of Colloid and Interface Science 293 (2006) 437–442.
[15] D.Amaranatha Reddy, A. Divya, G. Murali, R.P. Vijayalakshmi, B.K. Reddy, Synthesis and optical properties of Cr doped ZnS nanoparticles capped by 2-mercaptoethanol, Physica B 406 (2011) 1944–1949.
[16] Z. Chen, X.X. Li, N. Chen, G.P. Du, Y.S. Li, G.H. Liu, A.Y.M. Suen, Study on the optical properties of $Zn_{1-x}Mg_xS$ ($0 \le x \le 0.55$) quantum dots prepared by precipitation method, Materials Science and Engineering B 177 (2012) 337–340.
[17] C.S. Pathak, D.D. Mishra, V. Agarwala, M.K. Mandal, Blue light emission from barium doped zinc sulfide nanoparticles, Ceramics International 38 (2012) 5497–5500.
[18] T. Koda, S. Shionoya, Nature of the self-activated blue luminescence center in cubic ZnS:Cl single crystals, Physical Review 136 (1964) A541–A555.
[19] A.N. Georgobiani, R.G. Maev, Y.V. Ozerov, E.E. Strumban, Investigation of deep centres of chlorine-doped zinc sulfide crystals, Physica Status Solidi A 38 (1) (1976) 77–83.
[20] K. Akimoto, H. Okuyama, M. Ikeda, Y. Mori, Isoelectronic oxygen in II–VI semiconductors, Applied Physics Letters 60 (1992) 91–93.
[21] K. Manzoor, S.R. Vadera, N. Kumar, T.R.N. Kutty, Synthesis and photoluminescent properties of ZnS nanocrystals doped with copper and halogen, Materials Chemistry and Physics 82 (3) (2003) 718–725.
[22] M. Shirata, K. Shimizu, T. Koike, T. Komiyama, T. Matsui, Y. Nakanishi, K. Hara, Effect of Ir^{3+} incorporation on the luminescent properties of ZnS:Cl phosphors, Journal of The Electrochemical Society 158 (3) (2011) H318–H321.
[23] L.P. Wang, G.Y. Hong, A new preparation of zinc sulfide nanoparticles by solid-state method at low temperature, preparation of luminescent ZnS:Cu nanoparticles for the functionalization of transparent acrylate polymers, Materials Research Bulletin 15 (2000) 695–701.
[24] Z. Chen, S. Zhou, Y. Li, X.X. Li, Y. Li,W. Sun, G. Liu, N. Chen, G. Du, Strong blue luminescence of O^{2-} doped ZnS nanoparticles synthesized by a low temperature solid state reaction method, Materials Science in Semiconductor Processing, http://dx.doi.org/10.1016/j.mssp.2013.01.007, in press.
[25] Y. Li, S. Zhou, Z. Chen, Y.Yang, N. Chen, G. Du, Luminescence properties of Br-doped ZnS nanoparticles synthesized by a low temperature solid-state reaction method, Ceramics International, http://dx.doi.org/10.1016/j.ceramint.2012.12.064, in press.
[26] R.D. Shannon, Revised effective ionic radii and systematic studies of interatomie distances in halides and chaleogenides, Acta Crystallographica A 32 (1976) 751–926.
[27] J. Goldstein, D.E. Newbury, D.C. Joy, C.E. Lyman, P. Echlin, E. Lifshin, L. Sawyer, J.R. Michael, Scanning Electron Microscopy and X-ray Microanalysis, Springer, Berlin, 2003.
[28] K. Jayanthi, S. Chawla, H. Chander, D. Haranath, Structural optical and photoluminescence properties of ZnS:Cu nanoparticle thin films as a function of dopant concentration and quantum confinement effect, Crystal Research and Technology 42 (2007) 976–982.
[29] M. Salavati-Niasari, F. Davar, M.R. Loghman-Estarki, Long chain polymer assisted synthesis of flower-like cadmium sulfide nanorods via hydrothermal process, Journal of Alloys and Compounds 481 (2009) 776–780.
[30] J. Nanda, S. Sapra, D. Sarma, N. Chandrasekharan, G. Hodes, Size-selected zinc sulfide nanocrystallites: synthesis, structure, and optical studies, Chemistry of Materials 12 (2000) 1018–1024.
[31] A.A. Bol, A. Meijerink, Long-lived Mn^{2+} emission in nanocrystalline ZnS: Mn^2, Physical Review B 58 (1998) R15997–R16000.
[32] M. Lei, X. Fu, P. Li, W. Tang, Growth and photoluminescence of zinc blende ZnS nanowires via metalorganic chemical vapor deposition, Journal of Alloys and Compounds 509 (2011) 5769–5772.
[33] H. Lu, S. Chu, S. Tan, The characteristics of low-temperature-synthesized ZnS and ZnO nanoparticles, Journal of Crystal Growth 269 (2004) 385–391.
[34] J. Sun, E. Hao, Y. Sun, X. Zhang, B. Yang, S. Zou, J. Shen, S. Wang, Multilayer assemblies of colloidal ZnS doped with silver and polyelectrolytes based on electrostatic interaction, Thin Solid Films 327 (1998) 528–531.
[35] G. Dalpian, J. Chelikowsky, Self-purification in semiconductor nanocrystals, Physical Review Letters 96 (2006) 226802–226806.
[36] A.A. Bol, J. Ferwerda, J.A. Bergwerff, A. Meijerink, Luminescence of nanocrystalline ZnS:Cu^{2+}, Journal of Luminescence 99 (2002) 325–334.
[37] A. Bera, D. Basak, Photoluminescence and photoconductivity of ZnS-coated ZnO nanowires, Applied Materials and Interfaces 2 (2010) 408–412.